

Gas flow rates through inert and chemically active porous beds

Problem presented by

Heather Lawn, Jonathan Baker and John Curtis

AWE



ESGI100 was jointly hosted by

Smith Institute for Industrial Mathematics and System Engineering
Oxford

Smith *institute*
for industrial mathematics and system engineering



with additional financial support from
Engineering and Physical Sciences Research Council
European Journal of Applied Mathematics
Oxford Centre for Collaborative Applied Mathematics
Warwick Complexity Centre

Report authors

Peter D. Hicks (University of Aberdeen)
Maurizio Ceseri (IAC-CNR)

Executive Summary

The Atomic Weapons Establishment is interested in the behaviour of highly reactive chemical beds, in order to produce more reliable explosives. To improve understanding of the reaction evolution and bed mechanics the study group investigated the experiments of Goveas (1997), which involved the reaction of small beds of potassium picrate particles.

The study group developed a mechanistic model and used simplified analyses to investigate the reaction behaviour. The mechanistic model that was developed is able to explain the periodic chuffing observed in experiments, but does not rely on particle compaction. Two simplified analyses are undertaken, which support this mechanistic interpretation of the experiments. These simplified analyses calculate the reaction front speed based on a thermal analysis and the evolution of the gas bubble rising through the porous bed. The study group also suggest additional work that will further understanding of this phenomenon.

Version 1.1
June 13, 2014
iv+13 pages

Contributors

Jonathan Baker (AWE)
Alan Champneys (University of Bristol)
Joaquim Correia (University of Évora)
Maurizio Ceseri (IAC-CNR)
John Curtis (AWE)
Peter D. Hicks (University of Aberdeen)
John Hinch (University of Cambridge)
Andrew Lacey (Heriot-Watt University)
Heather Lawn (AWE)
John Ockendon (University of Oxford)
Colin Please (University of Oxford)
Michael Tsardakas (Heriot-Watt University)

Contents

1	Introduction	1
2	The problem	1
2.1	The experiments of Goveas (1997)	2
2.2	Other experimental evidence in the literature	3
2.3	Time and space scales in the experiment	4
3	Mechanistic interpretations	4
4	Governing equations	6
4.1	Non-dimensionalization	7
5	Model analysis	9
5.1	Analysis I: speed of reaction front	9
5.1.1	Problems with this explanation	10
5.2	Analysis II: pressurised gas bubble expelling and burning fuel (1D)	10
6	Conclusions and further work	11
	Bibliography	13
A	Properties of potassium picrate	13

1 Introduction

The Atomic Weapons Establishment (AWE) is interested in the behaviour of chemically active granular explosives such as potassium picrate and HMX. Once the ignition temperature of these substances is reached, the granules burn producing gas, heat and ash. An external source of oxygen is not required for the reaction to proceed and therefore the reaction rate is not limited by the availability of oxygen. The rapid generation of heat and gas in the pore spaces of a granular medium leads to high temperatures and pressures within the sample.

To investigate the properties of granular explosives, experimental tests have been conducted (see e.g. Baer et al., 1986; Goveas, 1997). In these tests small samples of explosive are confined by a metallic cylinder called a *squib*. Squib diameters are of the order of 5 mm, while heights range from 5 mm to a few centimetres. In squibs of small vertical height a deflagration front passes through the porous bed (Goveas, 1997), while in taller porous beds the deflagration front transitions to a detonation front before the chemical reaction reaches the surface (Baer et al., 1986).

For the study group, AWE are primarily interested in deflagration reactions in small squibs. In these cases the reaction is initiated by a heat source (either a heated wire or a laser), at the flat base of the squib. The other end of the squib may be open, covered with a thin plastic lid or be subject to stronger confinement. When present, the plastic lid is rapidly blown away in the early stages of the reaction due to the pressure build up in the gas occupying the bed pore spaces. This is followed by a plume of ash and also some unburnt granules. The squib is contained within a much larger safety box, allowing the products of the reaction to be safely monitored using high-speed photography.

A more detailed understanding of the reaction mechanics will enable AWE to design and produce more reliable explosives, while improving safety and reducing the risks of accidental detonation when using granular explosives.

This report reviews the work undertaken at the study group and includes: §2 a description of the problem and the available experimental results, §3 a mechanistic model that explains the reaction evolution, §4 an averaged continuum model for the behaviour of the particles and gas in a reactive porous bed and §5 two simplified analyses for the reaction front speed. The report concludes with suggestions for future modelling and experimental work on this problem.

2 The problem

The study group was tasked to investigate:

1. how gas flows through irregularly shaped particles, and whether the Kozeny-Carman equation (1) (relating the Kozeny-Carman constant K , porosity ϕ and specific surface area S_k), could be improved to extend the usual spherical particle geometries to account for cylindrical, tetrahedral, ellipsoid and rhombic particle geometries;
2. the critical pressure for the collapse of bed;

3. the rate of reaction and build up in pressure in energetic porous beds;
4. “chuffing” – a periodic phenomenon observed in the later stages of some experiments, thought to be due to incomplete ignition of reactants in the initial phase of the reaction.

The study group considers the first task to be ill-posed. The Kozeny-Carman equation

$$S_k = \sqrt{\frac{A_{\text{bed}}\phi^3\Delta p}{K(1-\phi)^2 L\eta q}}, \quad (1)$$

relating the cross-sectional area of a powder bed perpendicular to the flow A_{bed} , the pressure difference across the bed Δp , the vertical height of the bed L , the fluid viscosity η and the incompressible volumetric flow rate through the bed q ; is already an empirically determined law, which contains a fudge-factor - the Kozeny-Carman coefficient K .

The permeability of a porous bed is actually governed by shape of the voids separating the particles rather than the shape of the individual particles themselves. Therefore while it is potentially possible to consider the packing of a range of alternative particle geometries, the permeability is actually determined by the dust particles which collect between the large particles and constrict the fluid flow. Without knowledge of the dust occupying the pore spaces of the bed, the study group felt that improvements on the Kozeny-Carman equation were not possible, particularly given the Kozeny-Carman coefficient, a fudge-factor, which can already be used to fit a range of different experimental test cases.

The study group investigated tasks 2 – 4 via an analysis of a set of experiments conducted by Goveas (1997) into the reaction of small samples of potassium picrate. These experiments exhibit many of the important physical processes associated with this problem and form a good basis around which a detailed analysis can be undertaken.

2.1 The experiments of Goveas (1997)

Goveas (1997) experimentally investigated small samples of potassium picrate grains in a cylindrical metallic squib, which were prevented from falling out of the container by a thin plastic lid. The squib used had diameter 4.7 mm and height 6 mm, and was filled with one of two different grain sizes: 27 μm or 77 μm , leading to a range of different packing densities. The grains at the bottom metallic end of the squib were subsequently ignited by either a laser or a hot wire, while the subsequent ejecta from the top of the squib were monitored via high frame-rate camera. A typical sequence of the experimental images obtained is shown in figure 1.

Goveas (1997) observed a red flash from the bed when the experiment was conducted. This flash was not seen in any of the experimental video: presumably due to an inadequate frame rate of the high-speed photography. However, the study group considered this observation to be significant and after much debate the flash

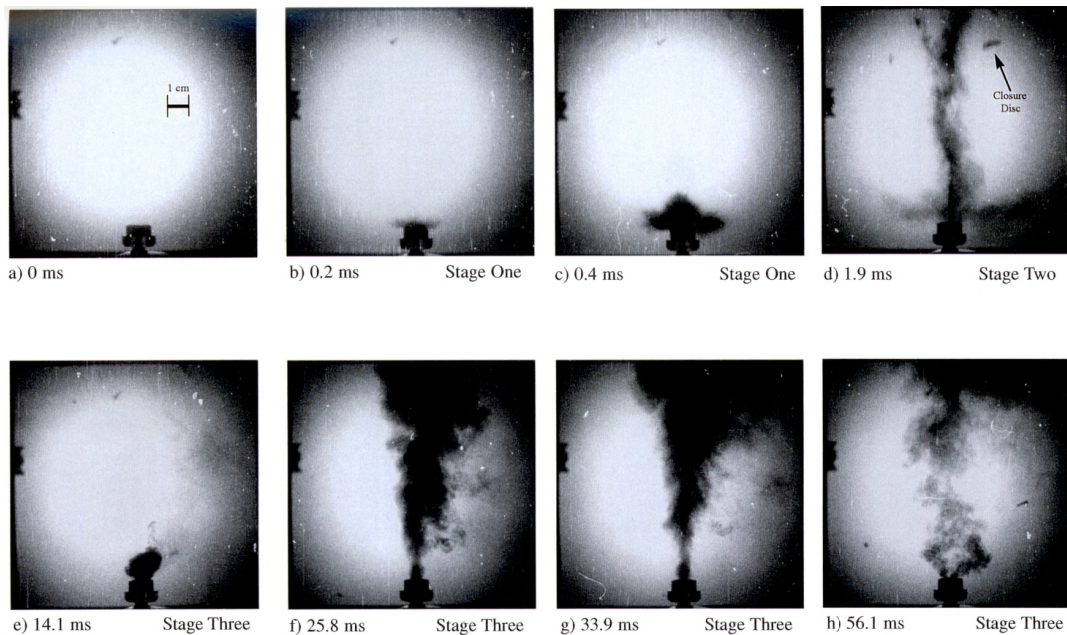


Figure 1: A sequence of frames from the video of a typical reaction (Goveas, 1997). The plastic lid of the squib is highlighted in sub-plot (d).

was inferred to be the deflagration flame exiting through the top of the particle bed. The red colour is indicative of a flame temperature of 700°C , and this value is used for the flame temperature in subsequent discussions.

2.2 Other experimental evidence in the literature

In addition to the Ph.D. thesis of Goveas (1997), the study group found several other experimental and modelling studies, which may go some way towards explaining the experimental results and answering the questions posed by AWE. The literature found by the study group can be broadly divided into two categories: studies of deflagration-to-detonation transition and studies of bubble growth with analogies to bubble behaviour in fluidized beds.

Examples of the former include the works of Baer et al. (1986) and Luebcke et al. (1995). In their experiments the squibs used had a larger vertical height, and unlike the experiments of Goveas (1997), the transition from a deflagration front to a detonation wave was observed prior to the reaction front reaching the top of the squib. These experiments also involved much more confined geometries surrounding the squib, and as a result of the confining geometry and a detonation reaction, pressures of 20000 MPa were measured, greatly exceeding the pressure predictions for the Goveas (1997) experiments.

The other strand of literature the study group looked at was bubbles rising within porous media and the craters formed when the bubble “bursts” at the surface. This situation was considered by some study group members to be analogous to a bubble rising within a fluidized bed. This problem was previously considered by

Knox and Terhune (1965).

2.3 Time and space scales in the experiment

Once the grains surrounding the heat source at the bottom of the squib reach the ignition temperature of roughly 300°C, a chemical reaction ensues, which is characterized by the equation



The reaction is exothermic deflagration, with the potassium picrate burning to produce gas, spent fuel in the form of ash and heat. The reaction is notable in that a source of gaseous oxygen is not required to allow the potassium picrate to burn. In the experiments of Goveas (1997), the deflagration front passes through the sample of potassium picrate before transition to a detonation front. However, in large porous beds detonation occurs and has been studied experimentally (Baer et al., 1986).

After the heat source is initiated at the base of the squib the deflagration flame passes through the sample in 1 ms and produces a red flash as the flame leaves the squib. This is followed immediately by plume of gas, ash and unburnt potassium picrate particles. By measuring the growth of the plume between consecutive frames in figure 1, an estimated plume speed of 100 ms⁻¹ was obtained. The study group obtained a wide range of predictions for the maximum pressure, ranging from 20 MPa to 100 MPa. The theory underlying these predictions is described in more detail in section 5.

The evolution of the experiment was found to depend on the porosity of the potassium picrate in the squib. Two different sample porosities ϕ of 40% and 20% were produced using the two different grain sizes. At the higher porosity, the sample density is lower and there is a larger void fraction through which the gas can flow. In this case all the reactants of the squib are burnt and ejected in the plume. The plume diameter equals the diameter of the squib. This behaviour is in marked contrast to the lower porosity case, where the sample density is higher and there are less void spaces through which the gas can flow. In this case the plume width is restricted to a 2 mm section in the middle of the squib, corresponding to about half the squib diameter. After the initial plume, the lower porosity experiments undergo a quiescent phase, before restarting with periodic, less energetic puffs ejecting burnt material and potassium picrate from the squib. The period of the chuffing is approximately 1 ms. The restarting of the reaction and chuffing is not observed in the higher porosity cases where all the potassium picrate is burnt in the initial plume.

3 Mechanistic interpretations

The study group proposed a mechanism for the reaction process, the stages of which are illustrated in figure 2. Starting with the top left sub-plot, the reaction is

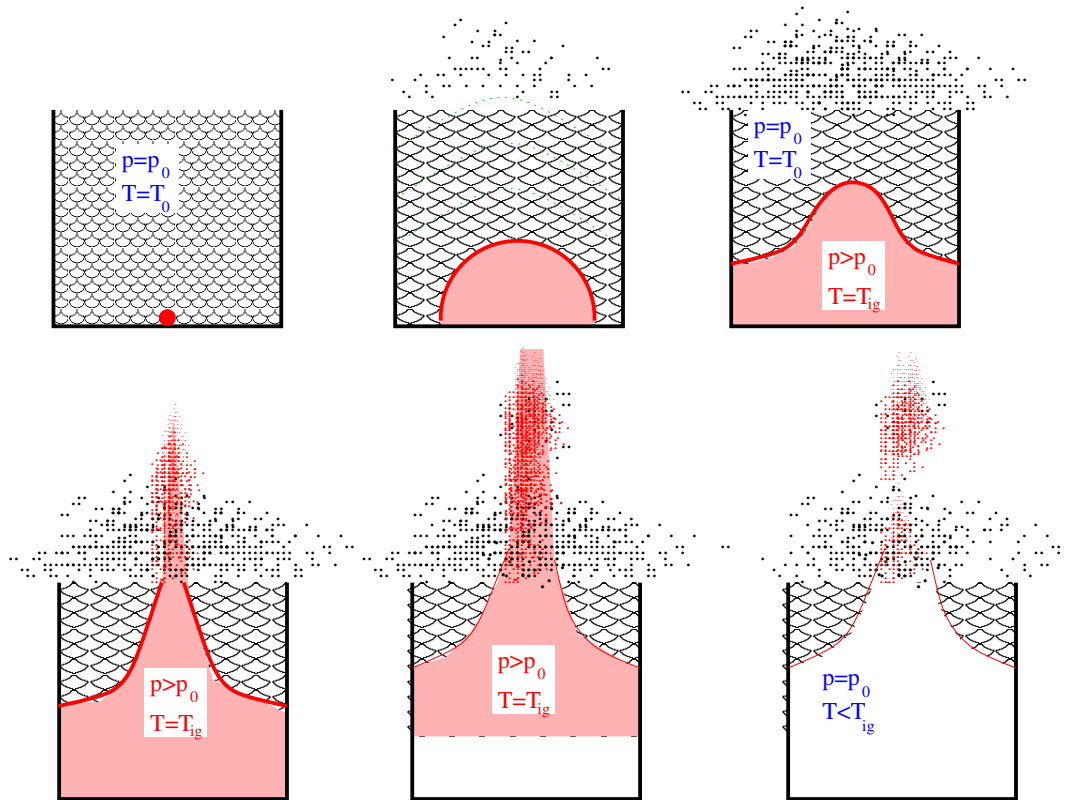


Figure 2: A sketch of the proposed stages of the reaction mechanism

initiated by a local heat source in the base of the squib. Once the particles reach the ignition temperature the reaction commences and an expanding deflagration front occurs. Gas and heat are produced at the deflagration front, leading to a pressure build-up and temperatures above ignition point behind the front.

This rapid burning and the corresponding reduction in particle volume results in elastic waves and particle-particle mechanical interactions throughout the squib. These waves travel through the squib much faster than the subsequent deflagration front and lead to dust particles and some potassium picrate particles being ejected from the squib. The mass of particles ejected in this phase is much lower than the mass of particles ejected in the subsequent plume, which occurs once the deflagration front reaches the surface of the porous bed.

The expanding deflagration front is constrained by the sides of the squib and consequently the study group suggest the deflagration front breaches the top of the squib before all the particles at the edges of the squib are burnt. A number of factors were suggested by the study group to explain the slower deflagration front progression near the sides of the squib including interactions between the localized ignition point and the squib geometry, and also friction between the particles and the squib walls.

Once the deflagration front breaks through the surface of the porous bed (as shown in the lower left sub-plot of figure 2), the burnt particles behind the front are

then rapidly ejected in the plume as a result of the large pressure build-up behind the front. At this point in the high porosity experiments, sufficient temperature and pressure remain to burn up the remaining potassium picrate in the squib, leading to all the material in the squib being ejected. However, for higher porosities the rapid normalization of pressure and temperature slows the remaining deflagration front and prevents all the potassium picrate particles being burnt up in the initial plume. A residual ring of particles remains around the rim of the squib. Further burning is then restricted to the surface of this unburnt rim of particles, with the production of heat and gas from this surface resulting in a periodic ejection of material driven by a cyclic release of gas. The study group believe this mechanism could produce the observed chuffing phenomenon.

4 Governing equations

In order to model the interactions of particles (with properties denoted by a subscript p), and gas (with properties denoted by a subscript g), the study group developed an averaged continuum model for the behaviour of the two phases. The phase density ρ , velocity \mathbf{u} and porosity ϕ are related via mass conservation equations, which in the gas and particle phases take the form

$$\frac{\partial}{\partial t} (\phi \rho_g) + \nabla \cdot (\phi \rho_g \mathbf{u}_g) = \Gamma, \quad (3a)$$

and

$$\frac{\partial}{\partial t} [(1 - \phi) \rho_p] + \nabla \cdot [(1 - \phi) \rho_p \mathbf{u}_p] = -\Gamma, \quad (3b)$$

respectively. Here an the Arrhenius reaction rate gives an inter-phase mass transfer

$$\Gamma = \rho_p (1 - \phi)^{2/3} A e^{E/RT}, \quad (3c)$$

where A is the reaction rate, E is the 1st order decomposition coefficient, R is the universal gas coefficient and T is the temperature, which is taken to be the same in both the gas and particle phase. In this expression the exponent of 2/3 on the term involving porosity assumes the reaction occurs at the particle surfaces rather than throughout their bulk.

The conservation of momentum in the gas phase implies

$$\frac{\partial}{\partial t} (\phi \rho_g \mathbf{u}_g) + \nabla \cdot (\phi \rho_g \mathbf{u}_g \mathbf{u}_g) = -\nabla (\phi p_g) - F, \quad (3d)$$

while assuming stresses cannot be transferred between particles, the conservation of momentum in the particle phase implies

$$\frac{\partial}{\partial t} [(1 - \phi) \rho_p \mathbf{u}_p] + \nabla \cdot [(1 - \phi) \rho_p \mathbf{u}_p \mathbf{u}_p] = F. \quad (3e)$$

Here p_g is the gas pressure. For high Reynolds number flow, the drag

$$F = \frac{\rho_g}{a} (\mathbf{u}_g - \mathbf{u}_p) |\mathbf{u}_g - \mathbf{u}_p|, \quad (3f)$$

where a is the typical particle length. A quadratic Forchheimer drag term is used, rather than a linear Darcy drag, as the gas Reynolds number is about 10 (based upon a typical gas velocity of 6 m s^{-1} , a particle length scale of $27 \mu\text{m}$), and will be larger still for the larger particle case. In practice one might expect that the gas inertia is small in comparison to the pressure-drag balance on the right-hand side of equation (3d). However, the terms on the left-hand side of equation (3d) are retained for numerical expediency and to allow for significantly higher than usual gas densities in the very high-pressure regions of the porous bed.

Assuming a common temperature for the gas and particle phases, energy conservation implies

$$\begin{aligned} \frac{\partial}{\partial t} [(\phi \rho_g c_{pg} + (1 - \phi) \rho_p c_{pp}) T] + \nabla \cdot [(\phi \rho_g c_{pg} \mathbf{u}_g + (1 - \phi) \rho_p c_{pp} \mathbf{u}_p) T] \\ = h\Gamma + \nabla \cdot (k \nabla T) - \phi p_g \nabla \cdot \mathbf{u}_g, \end{aligned} \quad (3g)$$

where c_p is a specific heat capacity, h is the latent heat of vaporisation and k is the thermal conductivity of the gas and particle mixture. Here the advection of heat (on the left-hand side), is balanced (on the right-hand side), by terms corresponding to heat generation by phase change, thermal diffusion and the work done compressing the gas.

The particle density ρ_p is assumed to be constant, so the system is completed by an equation of state for the gas phase, which is taken to be the ideal gas law

$$p_g = \frac{\rho_g R T}{m_g}, \quad (3h)$$

where m_g is the molecular mass of the gas produced. This system contains many parameters and properties of both the gas and the potassium picrate. Values for these properties are given in Appendix A.

4.1 Non-dimensionalization

The model of the previous section will now be reduced to its non-dimensional formulation. Let us consider the following rescaling:

$$\begin{aligned} \rho_g &= [\rho_g] \tilde{\rho}_g, & \mathbf{u}_g &= [\mathbf{u}_g] \tilde{\mathbf{u}}_g, & \mathbf{u}_p &= [\mathbf{u}_p] \tilde{\mathbf{u}}_g, & T &= [T] \tilde{T}, \\ t &= [t] \tilde{t}, & x &= L \tilde{x}, & p_g &= [p_g] \tilde{p}_g, \end{aligned}$$

where the characteristic variables are indicated by square brackets. In particular, we choose the vertical length L of the squib as the characteristic space variable, while the characteristic temperature is taken to be the flame temperature, 700°C .

Inserting the above quantities and dropping the tilde superscript to keep notation simple, we obtain from (3), the following rescaled system of equations:

Gas Conservation Equation

$$\frac{\partial}{\partial t} (\phi \rho_g) + \alpha_1 \nabla \cdot (\phi \rho_g \mathbf{u}_g) = \beta_1 (1 - \phi)^{2/3} e^{-\gamma_1 (\frac{1}{T} - 1)}. \quad (4a)$$

Particle Conservation Equation

$$\frac{\partial}{\partial t} (1 - \phi) + \alpha_1 \nabla \cdot [(1 - \phi) \mathbf{u}_p] = -\beta_2 (1 - \phi)^{2/3} e^{-\gamma_1 (\frac{1}{T} - 1)}. \quad (4b)$$

Gas Momentum Equation

$$\begin{aligned} \frac{\partial}{\partial t} (\phi \rho_g \mathbf{u}_g) + \alpha_1 \nabla \cdot (\phi \rho_g \mathbf{u}_g \mathbf{u}_g) = & \beta_3 \nabla (\phi p_g) \\ & - \frac{\alpha_1}{\delta_L} \frac{\rho_g}{(1 - \phi)^{2/3}} (\mathbf{u}_g - \mathbf{u}_p) |\mathbf{u}_g - \mathbf{u}_p|. \end{aligned} \quad (4c)$$

Particle Momentum Equation

$$\frac{\partial}{\partial t} [(1 - \phi) \mathbf{u}_p] + \alpha_1 \nabla \cdot [(1 - \phi) \mathbf{u}_p \mathbf{u}_p] = \frac{\delta_{\rho_g} \alpha_1}{\delta_L} \frac{\rho_g}{(1 - \phi)^{2/3}} (\mathbf{u}_g - \mathbf{u}_p) |\mathbf{u}_g - \mathbf{u}_p|. \quad (4d)$$

Energy Conservation Equation

$$\begin{aligned} \frac{\partial}{\partial t} [(\rho_g \phi \delta_\rho \delta_c + (1 - \phi)) T] + \alpha_1 \nabla \cdot [(\rho_g \phi \delta_\rho \delta_c \mathbf{u}_g + (1 - \phi) \mathbf{u}_p) T] \\ = \beta_1 \delta_\rho \gamma_2 (1 - \phi)^{2/3} e^{-\gamma_1 (\frac{1}{T} - 1)} \\ - \alpha_1 \gamma_3 \phi p_g \nabla \cdot \mathbf{u}_g + \beta_4 \nabla^2 T. \end{aligned} \quad (4e)$$

The non dimensional coefficients are defined as follows (assuming $[\mathbf{u}_g] = [\mathbf{u}_p] = [\mathbf{u}]$):

$$\begin{aligned} \alpha_1 &= \frac{[\mathbf{u}][t]}{L}, & \delta_\rho &= \frac{[\rho_g]}{\rho_p}, & \delta_L &= \frac{a}{L}, & \delta_c &= \frac{c_{pg}}{c_{pp}}, \\ \beta_1 &= \frac{\rho_p [t] A e^{-\gamma_1}}{[\rho_g]}, & \beta_2 &= \delta_\rho \beta_1, & \beta_3 &= \frac{[p_g][t]}{[\mathbf{u}]L[\rho_g]}, & \beta_4 &= \frac{k[t]}{\rho_p c_{pp} L^2}, \\ \gamma_1 &= \frac{E}{R[T]} & \gamma_2 &= h c_{pp} [T], & \gamma_3 &= \frac{[p_g]}{\rho_p c_{pp} [T]}. \end{aligned}$$

Here the characteristic pressure is given by the ideal gas law

$$[p_g] = \frac{[\rho_g] R [T]}{m_g},$$

and the nondimensional pressure is given as

$$p_g = \rho_g T.$$

We are interested here in evaluating the front propagation speed and the chemical reaction rate. The time scale of front propagation is given by imposing $\alpha_1 = 1$. Considering $[\mathbf{u}] = 100 \text{ m s}^{-1}$, this gives

$$[t_f] = \frac{6 \times 10^{-3} \text{ m}}{100 \text{ m s}^{-1}} = 6 \times 10^{-5} \text{ s}.$$

The chemical reaction characteristic time scale can be evaluated by taking $\beta_2 = 1$ or

$$[t_c] = \frac{e^{\gamma_1}}{A} = \frac{e^{21.2576}}{5.81 \times 10^{15} \text{ s}^{-1}} = 2.9369 \times 10^{-7} \text{ s}.$$

Thus chemical reactions do not appear to contribute substantially to front propagation since their speed is two orders of magnitude faster. In fact, choosing as characteristic time scale the value $[t_f]$, we have $\beta_2 = 218.48$.

Choosing a characteristic pressure of $[p_g] = 20 \text{ MPa}$, gives a characteristic gas density $n\rho_g = 660.45 \text{ kg m}^{-3}$, and a density ratio

$$\delta_\rho = \frac{[\rho_g]}{\rho_p} = \frac{660.45 \text{ kg m}^{-3}}{1500 \text{ kg m}^{-3}} = 0.44.$$

Since the particle to squib length scale ratio

$$\delta_L = \frac{a}{L} = \frac{2.7 \times 10^{-5} \text{ m}}{0.006 \text{ m}} = 4.5 \times 10^{-3},$$

the coefficient of the drag term on the right hand side of equation (4d), $\delta_\rho/\delta_L = 97.8$. This implies that $\mathbf{u}_g = \mathbf{u}_p$, indicating the particles and gas move with roughly the same speed.

The study group attempted to solve this system of equations numerically, but this was not possible over the course of the week. However, the study group believe that this system of equations is worthy of further investigation. In spite of this the study group were able to conduct simplified analyses based on these equations, which are described in the next section.

5 Model analysis

Over the course of the study group two different simplified models were investigated in order to understand the behaviour of the experiments. The aims of these analyses were to determine the speed of the reaction front and to determine the evolution of the pressurised gas bubble formed behind the reaction front.

5.1 Analysis I: speed of reaction front

The first analysis conducted by the study group involved solving the heat equation assuming the behaviour is driven by a balance between thermal conduction and the

heat of reaction. This analysis assumed that the reaction occurs on the surface of the particles and that there was a thin flame preceded by a pre-heat zone.

This model predicts a speed of the reaction front v_f , which is given by

$$v_f^2 = \frac{kRT_f^2 A}{\rho h E} e^{-E/RT_f},$$

where T_f is the flame temperature. Using a flame temperature of 700°C (as predicted by the red flash), and the properties given in Appendix A, this gives a velocity for the reaction front $v_f \approx 0.2 - 4 \text{ m s}^{-1}$. At this speed the reaction front would traverse the 6 mm height of the squib in $1.5 - 30 \text{ ms}$. However, this time is slower than the plume initiation time observed in the experiments, with the observed plume initiation time indicating that the actual front propagation speed is one order of magnitude greater than that given by this analysis.

One explanation for the slow predicted deflagration front velocity is that this analysis only considers the solid particles. In reality the surface reaction will jump across the void spaces reducing the transit time for the front. The front speed predicted by this analysis is therefore a lower bound on the actual transit speed, which should be approached in the limit of zero porosity.

5.1.1 Problems with this explanation

The second problem with this analysis is that behind the front the gas pressure is predicted to obtain values of 100 MPa. However, when the deflagration front reaches the surface of the squib, a pressure difference of this magnitude with the surrounding atmosphere would accelerate ejecta within the plume to velocities that are one order of magnitude larger than those observed.

This overly high pressure prediction is a consequence of assuming the particles and the gas phase have no motion until the plume erupts. This analysis should therefore be modified to incorporate particle and gas motion prior to the deflagration front reaching the top of the squib. The study group believe that the production of gas at the deflagration front and the subsequent motion of the gas and particles behind the deflagration front are analogous to a growing bubble rising up through a liquid. This similarity informed the second simplified model developed by the study group.

5.2 Analysis II: pressurised gas bubble expelling and burning fuel (1D)

The burning of potassium picrate and the production of gas is now considered in a simplified one-dimensional geometry. At time t the length of fuel remaining that can be burnt is denoted $L(t)$, with the burn velocity of the front v_f satisfying

$$\dot{L} = -v_f. \quad (5)$$

In this analysis the front speed or burn velocity is assumed to be constant, while in the gas bubble behind the front the density is denoted $\rho_g(t)$ and the pressure is denoted $p_g(t)$. The length of the one-dimensional bubble is $z(t)$.

The production of gas caused by burning particles is given by

$$\frac{d}{dt}(\rho_g z) = \rho_p v_f, \quad (6a)$$

while Newton's laws applied to the moving fuel gives

$$\frac{d}{dt}(\rho_p L(\dot{z} - v)) = p_g. \quad (6b)$$

The gas pressure can now be eliminated by the ideal gas law, which can be written as $p_g = \rho_g c^2$, for a sound speed $c = \sqrt{RT_f/m_g}$, which is taken to be constant. With the gas pressure expressed in this way

$$\frac{d}{dt}(L(\dot{z} - v)) = \frac{c^2 v_f t}{z}, \quad (7)$$

where the gas to particle density ratio has been determined by integrating the mass conservation equation.

The solution corresponding to a slow burn of the fuel (with $v_f \ll \dot{z}$ and L approximately constant), gives a prediction for bubble growth

$$\dot{z} = 3 \left(\frac{c^2 v_f t}{3L} \right)^{1/2}. \quad (8)$$

This corresponds to an accelerating front, with a lower pressure build-up than predicted by analysis 1, due to the movement of the fuel above the front.

6 Conclusions and further work

On behalf of AWE, the study group set out to improve understanding of the reaction dynamics of granular explosives. Four key problems were identified by AWE, which the study group considered via an analysis of the experimental results of Goveas (1997).

The first question posed by AWE - on whether the Kozeny-Carman equation can be improved for different shaped particles - was considered to be ill-posed. This is because permeability is largely dependent on the shapes of the smallest voids in sample rather than the shape of the particles themselves. Therefore the study group believe that improvement on the Kozeny-Carman equation is not possible, beyond fitting the Kozeny-Carman coefficient to match experimental results for porous beds of non-spherical particles.

Questions 2 through 4 relate to the dynamics of the reaction of a granular explosive. AWE suggested that particle compaction and bed collapse have a significant effect on the reaction dynamics. However, the study group developed a mechanistic model for the evolution of the reaction, which could produce the observed results, but did not rely on compaction of the porous bed. Therefore, while there may be cases where compaction is significant, the study group believes that the behaviour of the reacting porous bed can be explained without including this phenomenon.

The mechanistic model developed by the study group involves a deflagration front traversing the 6 mm height of the squib in 1 ms. This gives a typical velocity in the squib of 6 m s^{-1} , while behind the deflagration front there is a significant gas pressure build-up due to the production of gas at the front. The simplified analysis of the study group shows that the pressurized expansion of gas in the bubble accelerates the deflagration front through the squib.

When the front reaches the top of the squib, burnt and unburnt particles are ejected at 100 m s^{-1} . This enables a release of gas and reduces the pressure within the squib. In regions of the squib where the deflagration front has not yet reached the surface, the speed of the front slows down. In cases of high particle density and low porosity the deflagration front can stop, until a further pressure build-up occurs causing the front to advance. A subsequent release of pressure through the surface and a slowing of the front can produce the periodic chuffing observed in the experiments, as a result of a cyclic pressure build-up and deflagration front advance and halt in an annular region of unburnt particles surround the rim of the squib.

To improve understanding of this process the study group suggests that further analysis should be undertaken, particularly to analyse chuffing. This work should involve a further experimental campaign to assess the effect of distributive ignition and on the confinement of the squib. The study group believe gravity to be unimportant in the initial stages of a reaction and plume growth. However, this should also be tested, perhaps by conducting an experiment with the squib axis aligned perpendicular to gravity. In addition to improvements in high-speed photography since the original experimental campaign of Goveas (1997), careful measurements of velocity and pressure should be collected in any future to illuminate the process and to provide validation data for modelling. This additional experimental data should help with the development of analytical and numerical models (perhaps based on (3)), which should also be used to improve understanding of the reaction behaviour.

The study group would like to thank AWE for bringing this interesting and complicated problem to ESGI100, and hopes that the work undertaken during the meeting goes some way to illuminating the experiments, while suggesting pathways for further study in this area.

Bibliography

- Baer, M. R., Gross, R. J., Nunziato, J. W., and Igel, E. A. (1986). An experimental and theoretical study of deflagration-to-detonation transition (DDT) in the granular explosive, CP. *Combust. Flame*, 65, pp. 15–30.
- Goveas, S. G. (1997). *The Laser Ignition of Energetic Materials*. PhD thesis, Magdalene College, Cambridge.
- Knox, J. B. and Terhune, R. W. (1965). Calculation of explosion-produced craters – high-explosive sources. *J. Geophys. Res.*, 70 (10), pp. 2377–2393.
- Luebcke, P. E., Dickson, P. M., and Field, J. E. (1995). An experimental study of the deflagration-to-detonation transition in granular secondary explosives. *Proc. R. Soc. Lond. A*, 448, pp. 242–248.

A Properties of potassium picrate

Table 1: Properties of Potassium Picrate

Molecular mass	$m_g = 267.194 \text{ g mol}^{-1}$
Heat capacity	$c_p = 59.843 + 0.6807T - 3.589 \times 10^{-4}T^2 \text{ J mol}^{-1} \text{ K}^{-1}$
Density (crystal)	$\rho_c = 1.852 \text{ g cm}^{-3}$
Initial density of the bed	$\rho_p = 1.5 \text{ g cm}^{-3}$
Melting point	250°C
Ignition point	331°C
Particle size	24 μm - 74 μm
1st order decomposition coefficient	$E = 172 \text{ kJ mol}^{-1}$
Reaction rate	$A = 5.81 \times 10^{15} \text{ s}^{-1}$
Laser pulse duration	100 ms
Diameter of optical fibre	100 μm
Thermal conductivity (particles)	$k_p = 0.2 \text{ W m}^{-1} \text{ K}^{-1}$
Thermal conductivity (gas)	$k_g = 0.07 \text{ W m}^{-1} \text{ K}^{-1}$
Heat of reaction	$h = -681.68 \text{ kJ mol}^{-1}$